Refractive index and temperature sensor based on cladding-mode Bragg grating excited by abrupt taper interferometer

Shen Yang (杨 珅), Hao Sun (孙 浩), Liutong Yuan (袁柳通), Xiaolei Zhang (张晓蕾), Libin Zhou (周利斌), and Manli Hu (忽满利)*

Department of Physics, Northwest University, Xi'an 710069, China

**Corresponding author: huml@nwu.edu.cn*

Received July 2, 2013 accepted August 20, 2013; posted online December 9, 2013

A sensing structure consisting of an abrupt taper spliced uniformly in to a fiber Bragg grating (FBG) is proposed and experimentally demonstrates refractive index (RI) and temperature measurements. Cladding modes are generated in the fiber through the abrupt taper containing the FBG. Most modes are reflected by the FBG at shorter wavelengths and reenter the launch fiber after passing through the abrupt taper. Spectral integrals are used to measure the power generated by the cladding and core modes. A sensitivity of -83.97 nW/RIU for ambient RI and a temperature sensitivity of 10 pm/°C are obtained. No cross-sensitivity problems exist between ambient RI and temperature measurement.

OCIS codes: 060.2370, 060.3735, 280.6780.

doi: 10.3788/COL201311.120604.

Optical fiber refractive index (RI) sensors have been widely investigated in biological medicine and chemistry. Double-parameter measurement fiber sensors with various structures based on the fiber Bragg grating (FBG) and long period fiber grating (LPG) have been reported[1−4]. Normally, FBG is not sensitive to the RI of the surrounding environment. However, the removal of the FBG cladding facilitated the fabrication of a double-parameter measurement sensor based on FBG[5,6] or a coated polymer from the two sections of FBG[7]. The titled fiber grating can also be used to measure temperature and RI, because of the sensitivity of the excited cladding modes to temperature and RI. However, the core modes are only sensitive to temperature variation, contrary to LPG which is very sensitive to ambient RI. A number of studies on LPG have been reported, such as the fabrication of two-tandem LPG with different periods or the etching of one section of LPG and gold-plating of the other section[8,9]. Although this sensor can be used for double parameter measurement, it inevitably requires complex grating carving and special etching technologies, which increases the difficulty of sensor production.

Cross-sensitivity is a key issue in the practical application of optical fiber sensors, and temperature cross-sensitivity problems affect the precision of RI measurement[10−12]. Thus, a new technique should be developed to simultaneously measure the temperature and ambient RI with no cross-sensitivity issues.

We propose an optical fiber sensor that can simultaneously measure RI and temperature with no cross-sensitivity. The sensor comprises an abrupt taper and an FBG and only uses a single-mode fiber and an ordinary FBG to reduce difficulty in fabrication.

The structure of the sensor is shown in Fig. 1. A Corning SMF-28 fiber was used in this experiment, the fiber core/cladding diameter of the SMFis9/125 μm. The SMF core/cladding refractive index is 1.4502/1.445. Fujikura arc fusion splicer (FMS-60) was used to fabricate the sensor using a standard procedure. The DS-DS splice and 60-mm (FP-03) heating programs were used to taper the fiber. The following parameters programs were used: arcing time, 8000 ms; standard power, −20 bit; and motor moving distance, 125 μm. The taper had a waist diameter of 40 μm over an abrupt tapering length of 511μm. The maximum insertion loss was 3.5 dB, and the total length of the sensor was 2 cm. The taper section was fused at 10-mm upstream from the FBG. The FBG was fabricated using a phase mask technique with an argon ion laser, written in the SMF. The SMF-written FBG had a length of 10 mm, center wavelength of 1552.18 nm, 80% reflectivity, and a full-width at half-maximum (FWHM) bandwidth < 0.5 nm. The original grating spectrum can be affected by tapering the fiber. In this letter, the tapering fiber reduces the power of the original grating spectrum, but does not influence the wavelength of the original grating spectrum. The fraction of light that is coupled to the cladding depends on the taper length and depth. In the present case, these parameters were chosen to produce a high fringe visibility in the interferometric structure[13].

The abrupt taper partially excites the fundamental mode into the cladding[14]. The excited cladding modes recouples back to the core by the abrupt taper after reflection from FBG, from which the FBG causes modal interference as a result of the difference in the transmission constants between the core and cladding modes. This transmission is similar to that of a two-arm Michelson interferometer. The transmission result for this process takes the form

$$I = I_1 + I_2 + 2\sqrt{I_1 I_2}\cos\phi, \tag{1}$$

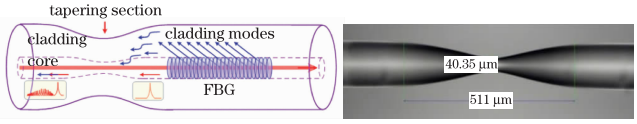

Fig. 1. (a) Schematic diagram of the sensor; (b) photograph of the electric-arc-heating induced abrupt-taper.

where $I_m(m = 1, 2)$ is the transmitted factor resulting from the coupling between the HE_{11} core mode and the HE_{1m} cladding mode, and ϕ is the phase difference that the HE_{11} and HE_{12} cladding modes have accumulated in the beating region[14].

A Michelson-type transmission formula (Eq. (1)) can be derived from all the modal interferometers. From this formula, the visibility is determined by the modal excitation and detection, with the phase ϕ given by

$$\phi = (\delta\beta)L, \tag{2}$$

where $\delta\beta$ is the difference between the two propagation constants, and L is the length of the beating region[15].

Light gradually expands upon transmissi to the taper, and the higher order cladding modes are excited and transmitted along the fiber cladding. The cladding modes are coupled into the fiber core and recoup led with the core mode. The reflective mode interference spectrogram is shown in Fig. 2.

The reflective power of the sensor is relative to the excitation rate of the cladding modes, the coupling ratio of cladding modes, and the transmittance of core mode that goes through the taper region. The cladding mode excitation rate and the core mode transmittance depends on the taper structure, the coupling ratio of cladding modes, and core mode dependent on the power of the cladding and core modes. The cladding mode field escapes from the cladding when the ambient RI changes because of the change in effective index of cladding modes. The power of the re-coupling cladding modes is likewise changed. Thus, the power of the cladding modes is related to the ambient RI. The FBG reflected power is only transmitted through the fiber core and is not influenced by the ambient RI, but is sensitive to temperature variation. When the environmental temperature increases by ΔT, according to the thermo-optic effect and thermal expansion (dn/dT and $d\Lambda/dT$) of the sensor, the drift in the reflected wavelength can be expressed as

$$\Delta\lambda = \lambda_0(\alpha_0 + \xi_0)\Delta T, \tag{3}$$

where α_0 is the fiber coefficient of thermal expansion (5.5×10^{-7} K^{-1}), and ξ_0 is the thermo-optical coefficient (6.67×10^{-6} K^{-1}). The resonance peak wavelengths offBG (i.e., the fiber core mode) and the cladding modes shift to a longer wavelength upon increase in temperature, but the mode field distribution is almost unchanged. Thus, the temperature variation slightly affects the reflected light[16].

The experimental setup for the RI and temperature measurement based on taper-FBG structure is illustrated in Fig. 3. A broadband source (BBS), an optical spectrum analyzer (OSA) with a resolution of 0.02 nm, and a temperature-controlled oven (DZ-3BC) were used. Complete details of all equipment used are listed in Table 1. The sensor was tightly fixed on a stage to avoid external strain and bending interference. The light from the BBS enters the circulator, goes through the sensor, and into the matching liquid. The light is reflected by FBG at the c-end, reenters the OSA.

The RI was measured at room temperature using the water-glycerin mixed solution. The RI ranges from 1.33 to 1.46, which is smaller than that of the fiber cladding. An Abbe refractometer was used to calibrate the RI of the solution before each measurement, and anhydrous ethanol was used to clean the sensing head after each measurement. The spectral response of the sensor to RI variation is shown in Fig. 4.

The power of the cladding mode decreases with increasing external RI, but the power of the coremode remains nearly unchanged (Fig. 4(a)). The spectral integral method was used to measure the powers of the cladding and core mode, and the results are shown in Fig. 4(b).

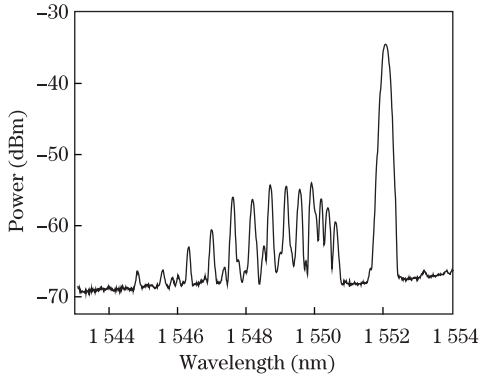

Fig. 2. Measured reflection spectrum of the sensor.

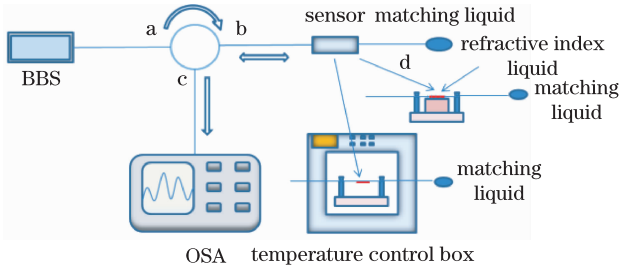

Fig. 3. Schematic diagram of the experimental setup for RI and temperature measurement.

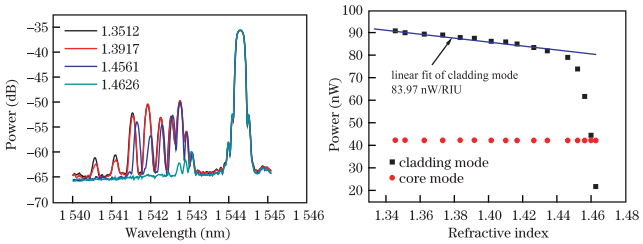

Fig. 4. (a) Spectral response of the sensor to RI variation; (b) powers of cladding and core modesdecrease with an increase in RI.

Table 1. Details of the Equipment Used

	OSA	AES Light Source	Temperature-Controlled Oven	Arc Fusion Splicer
Manufacturer	YOKOGAWA	LIGHTCOMM	TAISITE	Fujikura
Models	AQ6370B	C+L Band	DZ-3BC	FSM-60S

The power of the cladding mode decreases linearly with increasing RI that ranged from 1.34 to 1.44. By contrast, the power of the cladding mode decreases sharply when the external RI exceeds 1.44. However, the power of the core mode remains unchanged with RI variation. The RI sensitivity indicated by the variation in the power of the cladding mode is 83.97 nW/RIU, within the range from 1.34 to 1.44. The OSA power resolution is −90 dBm, so the RI resolution of the sensor is 0.00001 RI.

The signal stability of the sensor depends on the strength of the BBS stability when the power of the cladding mode is used as a sensor signal.The stability of the BBS is found to be merely+/−0.05 dB, so the error caused by instability of BBS need not be considered.

The drying process was used for the temperature-controlled oven. The sensor was placed in a temperature-controlled oven, and the sensor was allowed to be in the free state of elongation. During the process, the resonance peak wavelength of FBG, as well as the powers of the core and cladding modes, was measured every 5 °C from 30 to 70 °C. The sensor was left in the oven for 30 min, and the next measurement was performed after each 5 °C increase in the temperature. The reflection spectrum of the response to the temperature variation is shown in Fig. 5.

The reflection spectrum shifts to the longer wavelength with an increase in temperature (Fig. 5 and Eq. (3)). The power of the reflection spectrum is almost unchanged. The wavelength shift of the FBG with temperature variation was measured to determine the relationship between the reflection spectrum and temperature (Fig. 6).

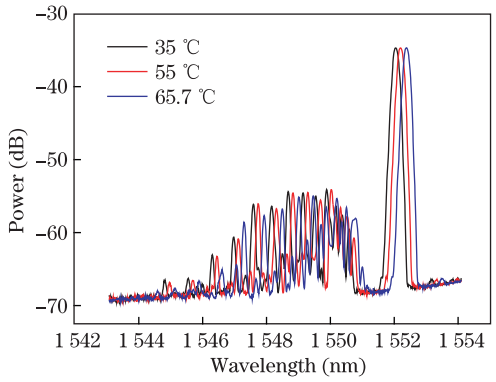

Fig. 5. Reflection spectrum with temperature variation.

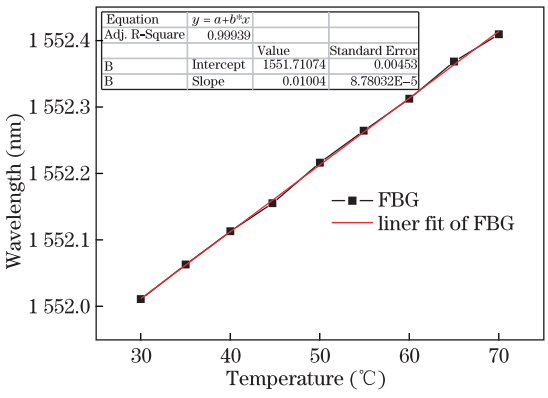

Fig. 6. Wavelength shift of FBG upon temperature variation.

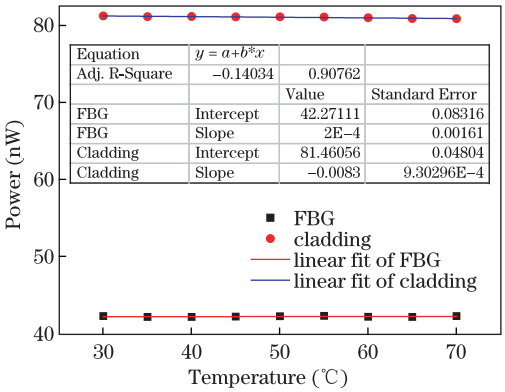

Fig. 7. Variations in the power of the core and cladding modes with temperature.

The relationship of the resonance wavelength shift with the temperature variation is shown in Fig. 6. The sensitivity is 10 pm/°C, and the linearity is 99.9%. The OSA wavelength resolution is 0.02 nm, so the temperature resolution of the sensor is 2 °C. The powers of the cladding and core modes were measured simultaneously to determine the possible cross-sensitivities of the temperature and the RI.

The power of the core mode remains unchanged upon temperature variation, but the power of the cladding mode decreases slightly with an increase in temperature, and the sensitivity is only 0.0083 nW/°C (shown in Fig. 7), compared with the RI sensitivity of 83.97 nW/RIU. Thus, the influence of temperature variation could be ignored. The power of the cladding mode may be used to reflect the change in RI, and at the same time, the wavelength shift in the FBG can reflect the variation in temperature. Thus, we can realize simultaneously two parameter measurements, namely, RI and temperature. Moreover, the error caused by stress and deformation can be solved using good encapsulation.

In conclusion, we propose an RI and temperature sensor on the basis of cladding mode recoupling. The sensor comprises an abrupt taper and flow with FBG. The compact structure has a total length of less than 20 mm and exhibits good linearity. The RI and temperature sensitivities of the sensor are 83.97 nW/RIU and 10 pm/°C, respectively, within the RI range from 1.33 to 1.44 and temperature range from 25 to 70 °C. Results show that almost no cross–sensitivities are found. Thus, RI and temperature measurement can be realized simultaneously through the measurement of the variation in the power of the cladding mode and the wavelength shift of FBG, respectively. The proposed sensor is easy to fabricate and does not require complex grating carving and optical fiber etching technologies, so it can be widely applied in biological medicine and chemistry.

This work was supported by the National Natural Science Foundation of China (Nos. 61377087 and 61077006), Shaanxi Province Natural Science Foundation Research Project (No. S2010JC3655), and Northwest University Postgraduate Innovative Talents Training Project (No. YZZ12085).

References

1. O. S. Wolfbeis, Anal. Chem. **76,** 3269 (2004).

2. M. P. DeLisa, Z. Zhang, M. Shiloach, S. Pilevar, C. C. Davis, J. S. Sirkis, and W. E. Bentley, Anal. Chem. **72,** 2895 (2000).
3. D. W. Kim, Y. Zhang, K. L. Cooper, and A. Wang, Electron. Lett. **42,** 324 (2006).
4. J. Huang, X. Lan, A. Kaur, H. Wang, L. Yuan, and H. Xiao, Opt. Eng. **52,** 014404 (2013).
5. P. Pilla, A. Iadicicco, L. Contessa, S. Campopiano, A. Cutolo, M. Giordano, G. Guerra, and A. Vusano, IEEE Photon. Technol. Lett. **17,** 1713 (2005).
6. Y. Cao, Y. Yang, X. Yang, and Z. Tong, Chin. Opt. Lett. **10,** 030605 (2012)
7. Y. Liu, L. Wang, M. Zhang, D. Tu, X. Mao, and Y. Liao, IEEE Photon. Technol. Lett. **19,** 880 (2007).
8. S. K. AbiKaedBey, C. C. Lam, T. Sun, and K. T. V. Grattan, Sens. Actuators. A **141,** 390 (2008).
9. X. Fang, C. Liao, and D. Wang. Opt. Lett. **35,** 1007 (2010).
10. P. Lu, L. Men, and Q. Chen, IEEE Sensor. J. **9,** 340 (2009).
11. C. Zhao, X. Yang, M. S. Demokan, and W. Jin, J. Lightwave Technol. **24,** 879 (2006).
12. T. Allsop, R. Neal, D. Giannone, D. J. Webb, D. J. Mapps, and I. Bennion, Appl. Opt. **42,** 3766 (2003).
13. O. Frazão, P. Caldas, F. M. Araújo, L. A. Ferreira, and J. L. Santos, Opt. Lett. **32,** 3074 (2007).
14. R. J. Black, S. Lacroix, F. Gonthier, and J. D. Love, IEEE. J. Opt. Electron. **138,** 355 (1991).
15. S. Lacroix, F. Gonthier, R. J. Black, and J. Bures, Opt. Lett. **13,** 395 (1988).
16. C. Gouveia, P. A. S. Jorge, J. M. Baptista, and O. Frazão, IEEE Photon. Technol. Lett. **23,** 804 (2011).